

Development of calcium stabilized nitrogen rich α -sialon ceramics along the $\text{Si}_3\text{N}_4:1/2\text{Ca}_3\text{N}_2:3\text{AlN}$ line using spark plasma sintering

B. A. AHMED^a, T. LAOUI^{b,c,*}, A. S. HAKEEM^{d,*}

^aDepartment of Mechanical Engineering, College of Electrical and Mechanical Engineering, National University of Sciences and Technology, Islamabad 44000, Pakistan

^bDepartment of Mechanical and Nuclear Engineering, University of Sharjah, Sharjah 27272, United Arab Emirates

^cCenter for Advanced Materials Research, Research Institute of Sciences and Engineering, University of Sharjah, Sharjah 27272, United Arab Emirates

^dCenter of Excellence in Nanotechnology, King Fahd University of Petroleum and Minerals, Dhahran 31261, Saudi Arabia

Received: April 5, 2020; Revised: June 9, 2020; Accepted: June 23, 2020

© The Author(s) 2020.

Abstract: Calcium stabilized nitrogen rich sialon ceramics having a general formula of $\text{Ca}_x\text{Si}_{12-2x}\text{Al}_{2x}\text{N}_{16}$ with x value (x is the solubility of cation Ca in α -sialon structure) in the range of 0.2–2.2 for compositions lying along the $\text{Si}_3\text{N}_4:1/2\text{Ca}_3\text{N}_2:3\text{AlN}$ line were synthesized using nano/submicron size starting powder precursors and spark plasma sintering (SPS) technique. The development of calcium stabilized nitrogen rich sialon ceramics at a significantly low sintering temperature of 1500 °C (typically reported a temperature of 1700 °C or greater) remains to be the highlight of the present study. The SPS processed sialons were characterized for their microstructure, phase and compositional analysis, and physical and mechanical properties. Furthermore, a correlation was developed between the lattice parameters and the content (x) of the alkaline metal cation in the α -sialon phase. Well-densified single-phase nitrogen rich α -sialon ceramics were achieved in the range of $0.53(3) \leq x \leq 1.27(3)$. A nitrogen rich α -sialon sample possessing a maximum hardness of 22.4 GPa and fracture toughness of $6.1 \text{ MPa}\cdot\text{m}^{1/2}$ was developed.

Keywords: nitrogen rich sialon ceramics; α -sialon; calcium sialons; spark plasma sintering (SPS); liquid phase sintering

1 Introduction

Sialon materials are a class of ceramics that have been thoroughly studied concerning their phase stability regimes, thermo-mechanical properties, photolumi-

nescence, and oxidation behavior [1–11]. Most of the studies on sialon ceramics have been concentrated around the two commonly known phases, namely α -sialon and β -sialon. A compound of silicon nitride, β -sialon having a general formula of $\text{Si}_{6-z}\text{Al}_z\text{O}_z\text{N}_{8-z}$, is formed as a result of the chemical replacement of silicon–nitrogen bonds with aluminum–oxygen bonds [12].

The compositions belonging to α -sialon phase are generally defined by $\text{M}_x^v\text{Si}_{12-(m+n)}\text{Al}_{m+n}\text{O}_n\text{N}_{16-n}$ (v re-

* Corresponding authors.

E-mail: T. Laoui, tlaoui@sharjah.ac.ae;

A. Hakeem, ashakeem@kfupm.edu.sa

presents valence of the cation M in α -sialon structure), where $x < 2$, $x = mv$, and $m(\text{Al-N})$ and $n(\text{Al-O})$ replace $(m+n)(\text{Si-N})$ bonds [13]. The substitution of silicon–nitrogen bonds with aluminum–nitrogen and aluminum–oxygen bonds results in a charge imbalance that is neutralized by the incorporation of M^{p+} ions such as Li^+ , Ca^{2+} , Mg^{2+} , Y^{3+} , and lanthanide ions [14–17]. Studies have been reported on the synthesis and phase stability regime of single phase α -sialons [14–19]. Several compositions of yttrium-stabilized α -sialons along the nitrogen rich line of $\text{Si}_3\text{N}_4\text{-YN:3AlN}$ were synthesized by Sun *et al.* [1] where the solubility limit of yttrium cation in α -sialon was found to be $0.43 < x < 0.8$. Huang *et al.* [14] studied the formation of oxygen rich yttrium stabilized α -sialons along the $\text{Si}_3\text{N}_4\text{-Y}_2\text{O}_3\text{:9AlN}$ and the solubility limit of yttrium cations was reported as $0.33 < x < 0.67$. It is well known that the synthesis of α -sialons occurs via a solution-reprecipitation mechanism, which involves the formation of an intermediary oxy-nitride liquid phase as a result of the reaction between the starting oxide and nitride precursors [20,21].

In contrast to α -sialons synthesized using yttrium or rare earth stabilizing cations, calcium stabilized α -sialons have gained considerable attention due to the higher solubility of calcium cation as compared to the former (the maximum solubility value x_{max} of 1.6 for Ca^{2+} as compared to x_{max} value of 1.0 for Yb^{2+}) [15,17]. Furthermore, Mandal and Thompson [22] studied on post sintering heat treatment of α -sialons, reported that in contrast to rare-earth stabilized α -sialons, calcium stabilized α -sialons depicted complete resistance towards α to β phase transformation in the temperature range of 1450–1500 °C.

The higher stability of calcium-stabilized α -sialons has been attributed to the lower valency of calcium cation, since the high-temperature stability of α -sialon

increases with increase in the solubility of charge stabilizing cation content (*ca.* Ca), which in turn increases with decrease in cation valency [23].

Figure 1 shows the Janecke prism and the calcium α -sialon plane highlighting the single-phase α -sialon region (oxygen rich as well as nitrogen rich) along with the neighboring phases at 1800 °C [24]. Several studies conducted on the synthesis of oxygen rich α -sialons have reported the formation of elongated morphology of α -sialon as compared to the generally known equiaxed morphology, and thus resulting in considerable improvement in the toughness of these materials [25–27]. However, there are very few studies that have been reported on the synthesis of nitrogen-rich α -sialons, mainly because they are challenging to densify [23,28]. Studies on the synthesis of calcium stabilized nitrogen rich α -sialons using all nitride precursors are even more scarce in the literature due to the difficulty in handling and storage of calcium nitride [23].

Xie *et al.* [23] worked on the synthesis of calcium stabilized nitrogen rich α -sialons along the $\text{Si}_3\text{N}_4\text{-1/2Ca}_3\text{N}_2\text{:3AlN}$ line at 1700 °C using the hot pressing (HP) technique. The limits of single phase calcium α -sialon was reported to be $0.5 < x < 1.7$. Later, Cai *et al.* [28] studied the synthesis of calcium stabilized nitrogen rich α -sialons using CaH_2 as a starting precursor instead of Ca_3N_2 at 1800 °C using HP technique. Single phase α -sialon ceramics were obtained in the range of $0.50 < x < 1.38$. Densification using conventional sintering processes, such as HP, is governed by the heat supplied via heating elements (comparatively much slower heating rate than SPS) and the externally applied pressure [29].

On the other hand, for the non-conventional and modern sintering process SPS, in addition to the uniaxial applied pressure, the pulsed nature of the current creates spark discharge. It gives rise to the joule heating

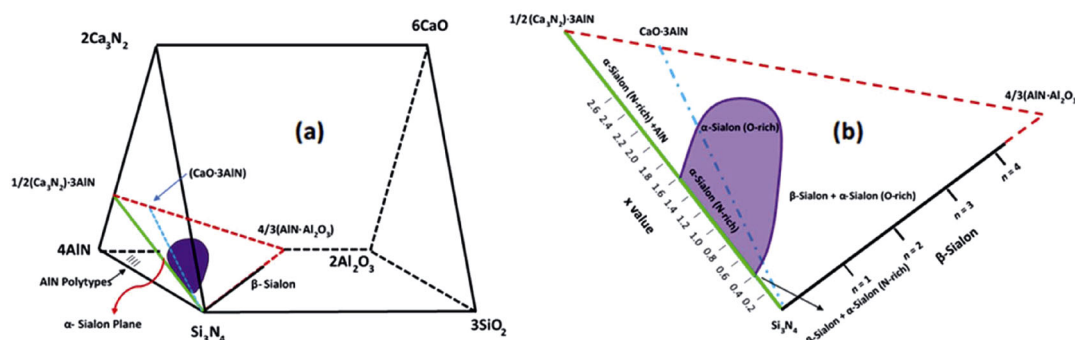


Fig. 1 Regenerated schematic representation of (a) Janecke prism of Ca-sialon system and (b) α -plane in Ca-sialon system at 1800 °C.

effect between the powder particles. The high rate of plasma discharge transmits and distributes the Joule heat throughout the material. This phenomenon results in a fast and uniform heat distribution within the sample, which ultimately leads to highly homogeneous samples with consistent densities. In addition, the high heating/cooling rate is beneficial as it restricts the grain growth as well as the formation of intermediate phase (s). Samples can be densified in a very short time by SPS [29,30]. Khan *et al.* [31] have reported the synthesis of oxygen rich calcium α -sialon ceramics at a relatively low temperature of 1500 °C using nano-sized precursors and SPS technique. However, to our knowledge, the synthesis of nitrogen rich sialons at low temperatures (below 1700 °C) has not been reported in the literature.

The present study aimed to develop calcium stabilized nitrogen rich α -sialons along the $\text{Si}_3\text{N}_4:1/2\text{Ca}_3\text{N}_2:3\text{AlN}$ line at a relatively low temperature of 1500 °C using SPS and nano-/submicron-size starting powder precursors. The developed sialons were characterized for their microstructure, phase and compositional analysis, and physical and mechanical properties. Furthermore, a correlation was developed between the lattice parameters and the content of alkaline metal cation (calcium) in the α -sialon.

2 Experimental

Calcium stabilized nitrogen rich α -sialon compositions having the general formula of $\text{Ca}_x\text{Si}_{12-m}\text{Al}_m\text{N}_{16}$ (where $x = m/2$), along the nitrogen rich line, were selected in this study. The nominal x value varied in the range of 0.2–2.2. Achievable compositions of α -sialon samples (by taking into account the oxide content on the powder surface) as listed in Table 1 were synthesized using starting powder precursors of α - Si_3N_4 with an average particle size of ~300 nm (UBE Industries SN-10, Japan), AlN with the particle size of ~50 nm (Chempur, Germany), and Ca_3N_2 of ~74 μm (~200 mesh, Sigma Aldrich, Germany). The oxygen content in the Si_3N_4 , AlN, and Ca_3N_2 powders corresponds to 2.87 wt% SiO_2 , 1.75 wt% Al_2O_3 , and 3.5 wt% CaO, respectively. The sample ID used in this manuscript starts with the letter ‘Ca’ followed by the nominal value of ‘ x ’ selected for the synthesis of a specific composition. For example, a sample having the chemical formula of $\text{Ca}_{0.2}\text{Si}_{11.6}\text{Al}_{0.4}\text{O}_{0.52}\text{N}_{15.31}$ is referred to as

Ca-0.2. Since Ca_3N_2 is very sensitive to moisture and air and quickly decomposes into calcium hydroxide and ammonia, powders of silicon nitride and aluminum nitride (required to synthesize 5 gm of a specific composition) were initially mixed via ultrasonic-probe sonicator in ethanol medium. The sonicated powder mixture was then dried in the oven at 95 °C for 24 h to evaporate ethanol. The dried powder mixture of silicon nitride and aluminum nitride was then mixed with the required amount of calcium nitride using mortar and pestle in NEXUS II glove box (Vacuum Atmosphere Company, USA) under the presence of high purity argon gas. The powder mixture thoroughly mixed for about 15–20 min was then poured into a 20 mm graphite die lined with BN, and the die was sealed with parafilm. The sealed die was taken out of the glove box and placed within the SPS chamber. The powder mixtures were synthesized (compacted and sintered) using an SPS apparatus (FCT system, model HP D5, Germany), calibrated and maintained by the manufacturer yearly. The schematic of the SPS machine is shown in Fig. 2. During the synthesis process, the temperature was monitored and controlled using a pyrometer, fixed just above the upper punch, measuring the temperature only 3 mm away from the top surface of powder mixture inside the graphite die. Moreover, as shown in Fig. 2, the temperature of the die was also measured using a K-type thermocouple, placed in the center of the die, only 3 mm away from the powder sample in the die. The maximum temperature difference of less than ± 20 °C, measured between pyrometer and thermocouple, assured the in-depth calibration.

Table 1 Starting compositions of calcium stabilized nitrogen rich sialons, along with sample ID, mole composition, and weight ratio

Sample ID	Starting Composition*	Ca_3N_2 (wt%)	Si_3N_4 (wt%)	AlN (wt%)
Ca-0.2	$\text{Ca}_{0.2}\text{Si}_{11.6}\text{Al}_{0.4}\text{O}_{0.52}\text{N}_{15.31}$	1.74	95.37	2.89
Ca-0.4	$\text{Ca}_{0.4}\text{Si}_{11.2}\text{Al}_{0.8}\text{O}_{0.52}\text{N}_{15.32}$	3.43	90.87	5.70
Ca-0.6	$\text{Ca}_{0.6}\text{Si}_{10.8}\text{Al}_{1.2}\text{O}_{0.52}\text{N}_{15.34}$	5.08	86.48	8.44
Ca-0.8	$\text{Ca}_{0.8}\text{Si}_{10.4}\text{Al}_{1.6}\text{O}_{0.52}\text{N}_{15.35}$	6.68	82.20	11.11
Ca-1.0	$\text{Ca}_{1.0}\text{Si}_{10}\text{Al}_{2.0}\text{O}_{0.51}\text{N}_{15.36}$	8.25	78.04	13.71
Ca-1.2	$\text{Ca}_{1.2}\text{Si}_{9.6}\text{Al}_{2.4}\text{O}_{0.51}\text{N}_{15.38}$	9.78	73.98	16.25
Ca-1.4	$\text{Ca}_{1.4}\text{Si}_{9.2}\text{Al}_{2.8}\text{O}_{0.51}\text{N}_{15.39}$	11.26	70.02	18.72
Ca-1.6	$\text{Ca}_{1.6}\text{Si}_{8.8}\text{Al}_{3.2}\text{O}_{0.50}\text{N}_{15.40}$	12.71	66.15	21.13
Ca-1.8	$\text{Ca}_{1.8}\text{Si}_{8.4}\text{Al}_{3.6}\text{O}_{0.50}\text{N}_{15.42}$	14.13	62.38	23.49
Ca-2.0	$\text{Ca}_{2.0}\text{Si}_{8.1}\text{Al}_{3.9}\text{O}_{0.50}\text{N}_{15.43}$	15.51	58.70	25.79
Ca-2.2	$\text{Ca}_{2.2}\text{Si}_{7.7}\text{Al}_{4.3}\text{O}_{0.50}\text{N}_{15.44}$	16.86	55.11	28.03

* Achievable compositions calculated by taking into account the oxide content in the starting powder precursors.

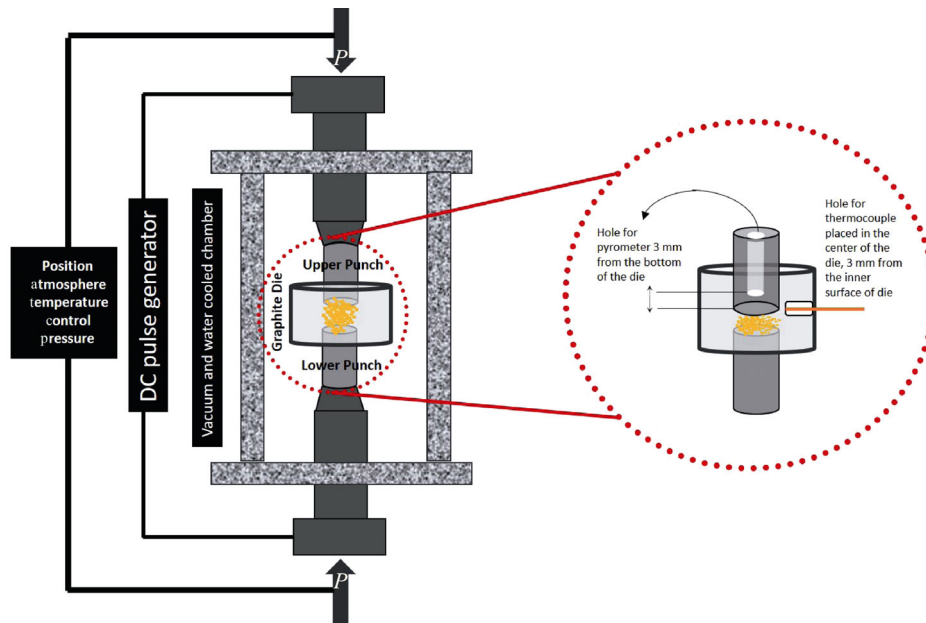


Fig. 2 Schematic of SPS equipment showing the die and temperature measurement configuration.

The powder mixture was consolidated into 20 mm diameter pellets at a synthesis temperature of 1500 °C with 30 min holding time in a vacuum environment and 50 MPa of constant uniaxial pressure. The heating rate of 100 °C/min was used in the synthesis, followed by a constant temperature holding process, then the samples were cooled down to room temperature (~22–25 °C) within 5 min. Each sample was prepared twice and densification data was obtained from the SPS equipment. The shrinkage curves were generated using the experimental data (relative piston displacement, time, and temperature values) collected and stored automatically on the FCT SPS software. The synthesized samples were cleaned of graphite using SiC grinding paper and were further ground and polished using Automet 300 Buehler grinding machine to a surface finish of 1 μm. Phase analysis was performed using Bruker D8 X-ray powder diffractometer with Cu Kα1 radiation ($\gamma = 0.15416$ nm). The tube current of 40 mA, accelerating voltage of 40 kV, step size of 0.02°, and step time of 3 s were maintained during the entire scan. In order to calculate the lattice parameters of α -sialon accurately, silicon powder was used as an internal standard. The amount of α - and β -phase was calculated using the following equation [32]:

$$\frac{I_{\beta}}{I_{\alpha} + I_{\beta}} = \frac{1}{1 + K \left[\left(\frac{1}{W_{\beta}} \right) - 1 \right]} \quad (1)$$

where I_{α} represents the observed intensity of (102) and

(210) peaks belonging to α -phase while I_{β} represents observed intensities of (101) and (210) peaks belonging to β -phase. W_{β} represents the fraction of β -phase while K is the proportionality constant (0.518 for β (101) and α (102) peaks while 0.544 for β (210) and α (210) peaks) [32]. The number of minor phases was determined based on the relative intensity method. Highly polished and fractured surfaces of the synthesized samples were observed using a field emission scanning electron microscope (FESEM, Lyra3, Tescan, Czech Republic) with an accelerating voltage of 20 kV. Phoenix focused ion beam (Helios G4 UX DualBeam, FEI) was used to prepare the lamellas for observation under a transmission electron microscope (TEM). High-resolution imaging and selected area diffraction patterns were acquired using FEI's Titan transmission electron microscope equipped with an energy dispersive X-ray (EDX) detector. Five area EDX analyses were performed to calculate the cation composition. The software UnitCell-Win and XRD peak positions were used to calculate the lattice parameters. The density of the synthesized disk-shaped samples (after removal of graphite) was calculated using Archimedes' principle. Vickers hardness (HV_{10}) was measured on the surface of the polished samples using a universal hardness tester (Zwick-Roell, ZHU250, Germany). The indentation load of 10 kg was adopted for the hardness test. The indentation method was used to calculate the fracture toughness (K_{IC}) of the synthesized samples [33–36]. Evan's equation shown below was used to calculate the

indentation fracture toughness.

$$K_{IC} = 0.48 \left(\frac{MCL}{d/2} \right)^{-1.5} \left(\frac{HV_{10} \sqrt{d/2}}{3} \right) \quad (2)$$

where MCL stands for the maximum crack length initiated from the indentation and d is the average diagonal.

3 Results and discussion

3.1 Synthesis and densification behavior

The densification behavior of the samples synthesized over the range of $0.2 < x < 2.2$ is shown in Fig. 3 (the inset shows the complete densification curves), where the ordinate represents the displacement of an upper punch of the die in mm, depicting the shrinkage, and the abscissa represents the synthesis/sintering time. It is observed that with the increase in the x value, denoting the increase in Ca content, the shrinkage curve shifts to the left (towards shorter time). Samples having higher x value exhibit a more significant shrinkage (larger displacement) and subsequently are more densified than at the earlier stage of synthesis. It is quite known that the densification of silicon nitride-based materials involves the formation of a transient liquid phase, where the densification behavior depends on the viscosity, amount, and wetting characteristic of the transient liquid phase. In the case of the calcium stabilized α -sialons synthesized using oxide additives, the formation of the transient liquid phase takes place as a result of the reaction between silicon oxide present on the surface of silicon nitride powder and oxide additives. In our case, there are two sources of a liquid phase. Firstly, due to the eutectic reaction between silicon oxide, aluminum oxide, and calcium oxide present on the surfaces of starting nitride precursors, and secondly due to the melting of calcium nitride which takes place at about 1195 °C (since calcium nitride is not used as a starting precursor in the synthesis of oxygen rich calcium α -sialons) [37]. Furthermore, since the oxide rich eutectic liquid phase is produced as a result of the surface oxide layer present on the surface of starting nitride precursors, the amount of oxide rich transient liquid is very small. On the other hand, the amount of nitrogen liquid phase formed because of the melting of calcium nitride increases, with the increase in x value (more calcium nitride) and consequently resulted in easier densification (higher shrinkage within a shorter time) of the samples

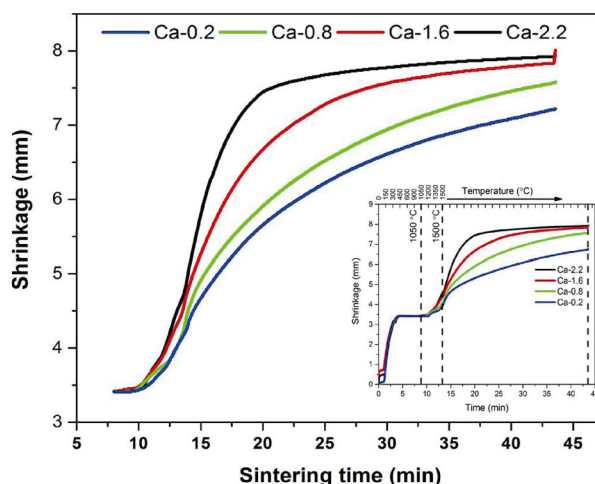


Fig. 3 Densification curves of several compositions of calcium stabilized nitrogen rich sialons synthesized at 1500 °C using SPS technique, where Ca content varies between 0.2 and 2.2. The inset shows the complete densification curves and the main plot represents the selected high-temperature region (heating from 1050 to 1500 °C followed by 30 min holding time).

having high x value. Xie *et al.* [23] reported a similar trend for the nitrogen rich α -sialons synthesized using HP technique and micron size precursors at 1700 °C and 1 h holding time. However, the reported shrinkage rate was much slower due to the slower reaction kinetics as a result of the conventional heating technique (slower heating rate) as well as due to larger size ($> 1 \mu\text{m}$) of the starting powder precursors.

Table 2 shows the density values of the nitrogen rich calcium stabilized α -sialons for compositions having x values in the range of 0.2–2.2, synthesized at a relatively low temperature of 1500 °C. The density of the samples synthesized at 1500 °C was measured to be in the range of 2.96–3.21 g/cm³ and was seen to increase with the increase in x value (increase in Ca₃N₂ content). Xie *et al.* [23] reported comparable density values (3.10–3.15 g/cm³) with a similar trend for the nitrogen rich α -sialons synthesized at 1700 °C using HP technique and micron size precursors. Cai *et al.* [28] worked on the synthesis of calcium stabilized nitrogen rich α -sialons at 1800 °C using HP technique. The observed density values were reported to be in the range of 3.16–3.26 g/cm³. Furthermore, Wang *et al.* [38] reported density values of 3.07 and 3.17 g/cm³ at 1700 and 1750 °C, respectively, for dense hot-pressed oxygen rich calcium α -sialon having a composition of Ca_{0.5}Si_{10.5}Al_{1.5}O_{0.5}N_{15.5}. Xie *et al.* [23] communicated a failure to synthesize well-densified yttrium stabilized nitrogen rich α -sialons along the Si₃N₄:YN:3AlN

Table 2 Density of calcium stabilized nitrogen rich α -sialon sintered at 1500 °C

Sample ID	Ca-0.2	Ca-0.4	Ca-0.6	Ca-0.8	Ca-1.0	Ca-1.2	Ca-1.4	Ca-1.6	Ca-1.8	Ca-2.0	Ca-2.2
x	0.2	0.4	0.6	0.8	1	1.2	1.4	1.6	1.8	2	2.2
Density (g/cm ³)	2.96	3.06	3.09	3.14	3.17	3.17	3.18	3.19	3.20	3.20	3.21

where an insufficient amount of liquid phase was provided to be the main reason. This suggests that along with nano-size starting precursors and novel pulsed-based SPS technique, low melting temperature (1195 °C) of calcium nitride plays a pivotal role in achieving well-densified samples at 1500 °C. It has been reported in the literature that a small particle size of starting powders helps to synthesize dense sialon materials at low temperatures [39,40].

3.2 Phase analysis

Figure 4 shows X-ray diffraction (XRD) patterns of the samples synthesized at 1500 °C. The single phase calcium stabilized α -sialon phase is observed for samples produced in the range of $0.6 \leq x \leq 1.4$ (Ca-0.6 to Ca-1.4). Dual phases (α - and β -sialons) are observed for samples having $x \leq 0.4$, where the amount of β -sialon phase is seen to decrease as the composition shifts towards single phase α -sialon. Beyond the single-phase region, α -sialon coexists with AlN and CaSiAlN₃ in the range of $1.6 \leq x \leq 2.0$. Figure 5(a) displays the regenerated schematic representation of α -plane in Ca-sialon system showing phase stability regime region along the N-rich line at 1500 °C where Fig. 5(b) represents the same, the orientation of the α -plane is the one which is most commonly presented in the literature. A similar observation is reported by Xie *et al.* [23] for the calcium stabilized nitrogen rich samples synthesized at 1700 °C using HP technique. Furthermore, Cai [24] have also communicated the formation of AlN and CaSiAlN₃ phases along with α -phase for higher values of x (1.6) on the synthesis of nitrogen rich sialons at 1800 °C and the single phase α -sialon phase is reported to be in the range of $0.6 \leq x \leq 1.6$.

XRD results of the samples synthesized at 1500 °C are summarized in Table 3. Lattice parameters of α -sialon are seen to increase with the increase in x value attributed to the fact that more amount of Si–N bonds are replaced by Al–N bonds as well as more amount of calcium ion is being incorporated in the α -sialon. In calcium stabilized α -sialons, the charge imbalance caused as a result of the substitution of Si⁴⁺ for Al³⁺ is

brought into balance by the addition of Ca²⁺ ions at the interstitial positions in the network. It is established that α -sialon unit cell contains two interstices per unit cell, the upper solubility limit of calcium ion(s) in α -sialon having a composition of Ca₂Si₈Al₂N₁₆ is ideally believed to be 2. However, due to the unavoidable presence of the oxide layer on the surface of starting precursors, this composition has not been achieved so far. Cai *et al.* [28] have reported a maximum achieved solubility limit of 1.82 for a nominal x value of 2.2 on the synthesis of nitrogen rich sialons at 1800 °C. Similarly, Xie *et al.* [23] reported the maximum solubility value of 1.7 for the calcium stabilized nitrogen rich samples synthesized at 1700 °C using HP technique. In our case, the maximum solubility limit has been determined to be 1.83 for the nominal x value of 2.2.

Figure 6 shows the variation of α -sialon lattice parameters with respect to change in x value. Similar behavior is reported by Cai [24] for samples synthesized at 1800 °C (Fig. 6). The following empirical relationships can well define the dependence of α -sialon lattice parameters with the amount of Ca²⁺:

$$a = 0.0949x + 7.7605 \text{ (\AA)} \quad (1)$$

$$c = 0.0680x + 5.6326 \text{ (\AA)} \quad (2)$$

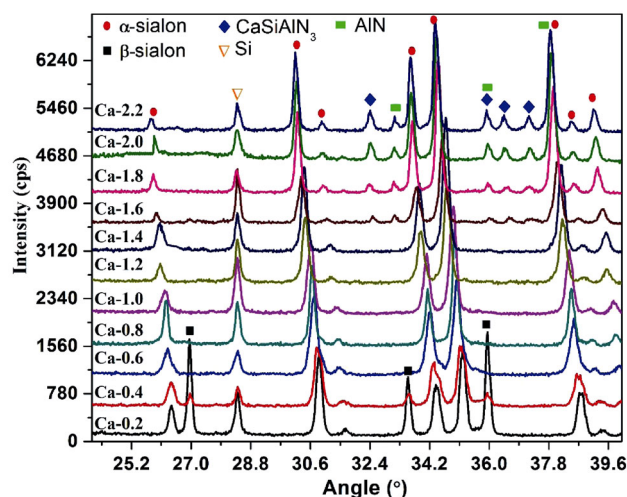


Fig. 4 XRD patterns of the calcium stabilized nitrogen rich α -sialon samples synthesized along the Si₃N₄:1/2Ca₃N₂:3AlN line at synthesis temperature of 1500 °C.

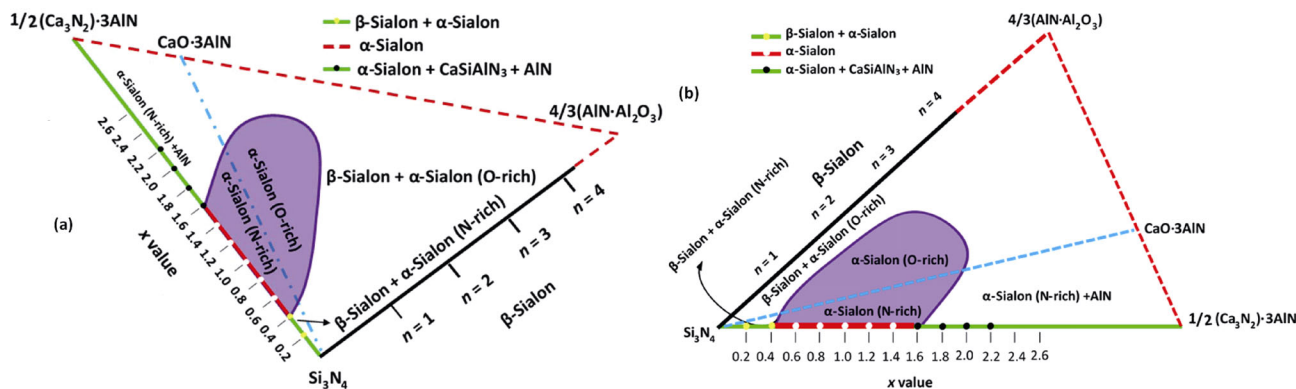


Fig. 5 (a) Regenerated schematic representation of α -plane in Ca-sialon system showing phase stability regime along the N-rich line at 1500 °C and (b) another representation where the orientation of the α -plane is one which is most commonly in the literature.

Table 3 Lattice parameters, mechanical properties, and phase assemblage of calcium stabilized nitrogen rich sialons synthesized at 1500 °C

Sample ID	x (Ca)		Lattice parameters		HV_{10} (GPa)	K_{IC} (MPa·m ^{1/2})	Phase assemblage (wt%)
	Nom	EDXS	a (Å)	c (Å)			
Si ₃ N ₄ [*]	0	—	7.7541	5.6217	—	—	—
Ca-0.2	0.2	0.15(2)	7.7814(6)	5.6490(4)	18.5 (3)	4.5 (4)	α (61), β (39)
Ca-0.4	0.4	0.33(3)	7.7971(6)	5.6593(4)	19.4 (7)	5.0 (4)	α (87), β (13)
Ca-0.6	0.6	0.53(3)	7.8210(7)	5.6631(5)	22.2 (2)	5.6 (3)	α (100)
Ca-0.8	0.8	0.73(3)	7.8343(7)	5.6885(5)	22.4 (5)	5.7 (3)	α (100)
Ca-1.0	1.0	0.84(4)	7.8470(7)	5.7011(5)	21.8 (4)	5.7 (3)	α (100)
Ca-1.2	1.2	1.01(5)	7.8770(7)	5.7153(4)	21.6 (2)	5.3 (2)	α (100)
Ca-1.4	1.4	1.27(3)	7.8937(7)	5.7316(5)	21.0 (3)	6.1 (3)	α (100)
Ca-1.6	1.6	1.39(4)	7.9170(7)	5.7464(5)	20.8 (4)	5.8 (2)	α (82), A (10), C (8)
Ca-1.8	1.8	1.54(5)	7.9320(6)	5.7583(5)	20.1 (7)	5.5 (3)	α (82), A (9), C (9)
Ca-2.0	2.0	1.68(4)	7.9534(7)	5.7695(5)	19.3 (6)	5.7 (2)	α (79), A (10), C (11)
Ca-2.2	2.2	1.83(5)	7.9651(6)	5.7790(4)	18.7 (5)	5.2 (3)	α (75), A (12), C (13)

^{*}JCPDS 41-0360, nominal (nom), energy dispersive X-rayspectrometer (EDXS), aluminum nitride (JCPDS 25-1133) (A), CaSiAlN₃ (JCPDS 39-747) (C).

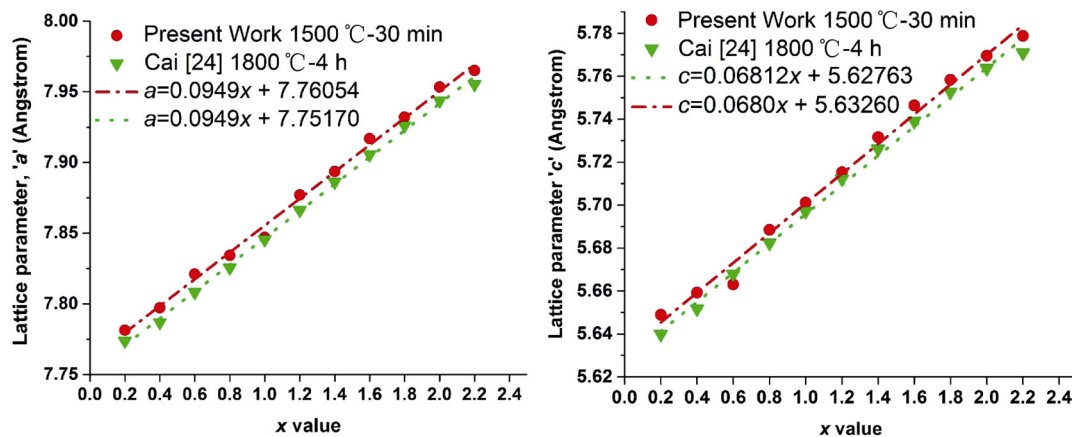


Fig. 6 Variation of lattice parameters of calcium stabilized nitrogen rich α -sialons with x value for samples synthesized at 1500 °C using SPS and those reported by Cai [24] at 1800 °C using HP.

Formation of α -sialon phase for a sample having x value as low as 0.2, along with the observation suggesting a linear dependence of α -sialon unit cell parameters with x value, provides a good reason to believe that calcium stabilized nitrogen rich α -sialon forms continuously in the range of $0 < x < 1.83$. Therefore, previously reported low solubility limit of Ca^{2+} in α -sialons, should not be presented as a structural limitation. Rather, the formation of single phase α -sialons near the nitrogen rich corner has not been attained due to the presence of the oxide layer contamination leading to the formation of β -sialon phase.

3.3 Microstructure analysis

Figures 7(a)–7(f) depict the secondary electron FESEM micrographs of the fractured surface of samples from the nitrogen rich sialon ceramics sintered at 1500 °C. Primarily, a classical intergranular fracture was observed in all samples, along with some amount of grain pullout. Sample Ca-0.2 containing α - and β -sialon phases exhibit elongated morphology of β -sialon along with smaller equiaxed grains of α -sialon (Fig. 7(a)). Samples

with x values greater than 0.4 (Ca-0.6 to Ca-2.2) composed of single phase or almost single-phase nitrogen rich calcium α -sialon depicted fine equiaxed grains (a morphology typical of α -sialon phase). However, with the increase in x value (more Ca_3N_2), α -sialon grains with elongated morphology are also observed. Additionally, it is observed that an increase in x value yields an increase in the average grain size of α -sialon. The grain size distribution for the three samples (Ca-0.6, Ca-1.2, and Ca-2.0) is depicted in Fig. 8 where the average grain size is measured to increase from 286 ± 98 to 385 ± 96 and 468 ± 169 nm, respectively.

Figures 9(a)–9(e) show the low and high-resolution TEM images of the microstructures of nitrogen rich calcium α -sialon samples (having the ID as Ca-0.6, Ca-1.2, and Ca-2.0). In accordance with the observations made on fractured surfaces, sample Ca-0.6 displays an equiaxed morphology of α -sialon grains with an average grain size of 277 ± 34.56 nm. For samples Ca-1.2 and Ca-2.0, a dual morphology of α -sialon grains, i.e., elongated grains alongside the equiaxed grains, is observed. The average size of the grains is

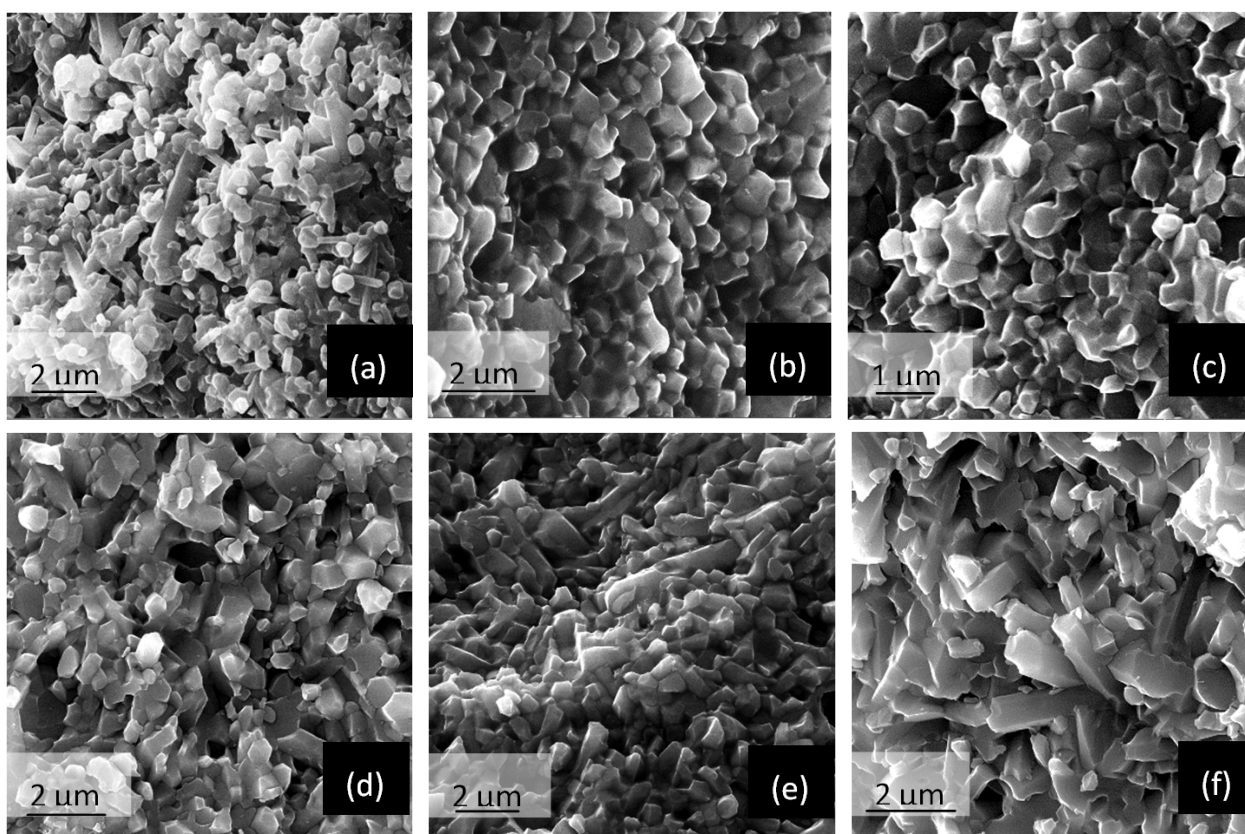


Fig. 7 Secondary electron (FESEM) micrographs of the fractured surfaces of nitrogen rich samples synthesized at 1500 °C using different x values: (a) Ca-0.2, (b) Ca-0.6, (c) Ca-1.2, (d) Ca-1.6, (e) Ca-1.8, and (f) Ca-2.0.

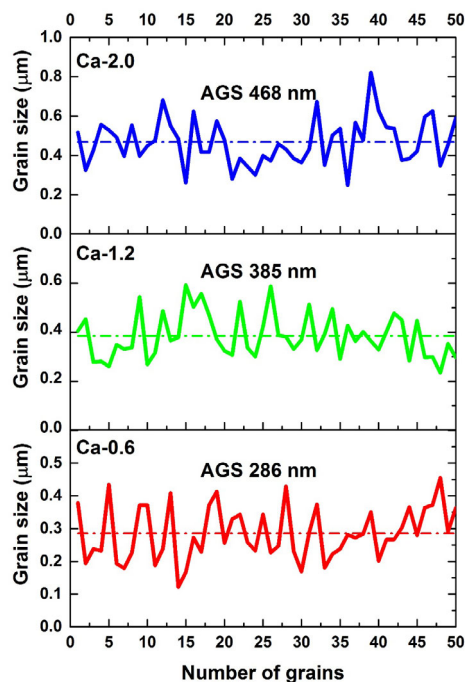


Fig. 8 Grain size distribution of nitrogen rich samples synthesized at 1500 °C having the sample ID of Ca-0.6, Ca-1.2, and Ca-2.0.

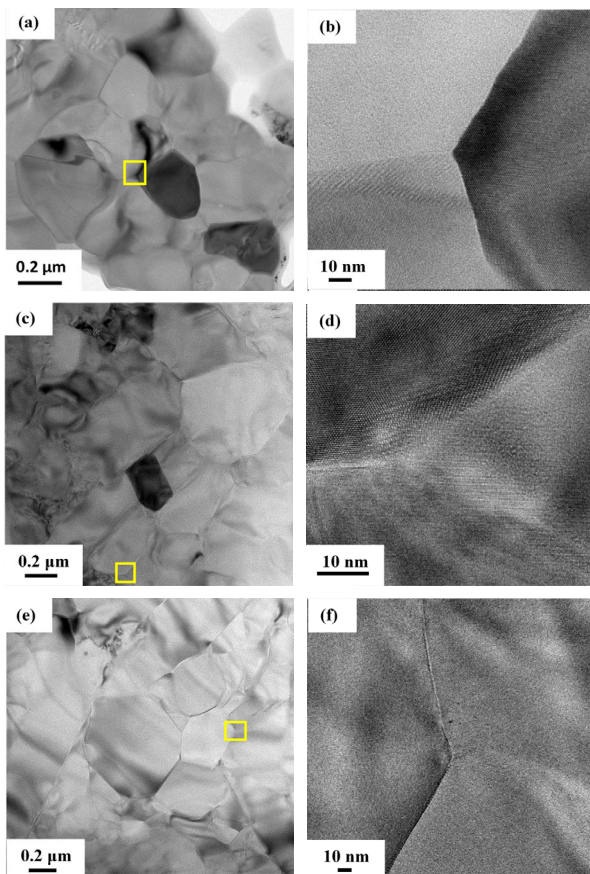


Fig. 9 Low and high resolution TEM micrographs of the nitrogen rich samples synthesized at 1500 °C using different x values: (a, b) Ca-0.6, (c, d) Ca-1.2, and (e, f) Ca-2.0.

measured to be 386 ± 127 nm for Ca-1.2 and 449 ± 142 nm for Ca-2.0, respectively. The α -sialon ceramics having an elongated morphology as a result of preferential grain growth during the densification process has also been reported in the synthesis of hot-pressed oxygen rich Ca- α -sialons [11,38,41]. It is known that the grain growth of α -sialon takes place via solution and re-precipitation mechanism, and the presence of a liquid phase is necessary to promote grain growth. Therefore, the presence of elongated morphology of α -sialon grains as well as the grain growth for samples having higher x value (i.e., more Ca_3N_2) may well be attributed to the formation of a higher amount of transient liquid phase. Thorel *et al.* [42] studied on high-temperature mechanical properties and intergranular structure of sialons (oxygen rich) and reported that intergranular phase (if present) is always amorphous and can exist as reasonably large pockets having a size in the range of 0.1–1 μm or interfacial glassy film with a minimum reported thickness of about 60 nm. In our study, the high-resolution TEM images of nitrogen rich sialons (Figs. 9(b), 9(d), and 9(e)) reveal that there is no sign of a glassy phase present at the grain boundaries nor at the junction of multiple grains. These results suggest that the synthesized nitrogen rich sialons would be more stable at high temperatures (1400–1600 °C) compared to the oxygen rich sialons containing an amorphous phase on the grain boundaries.

3.4 Mechanical properties

HV_{10} and K_{IC} of the calcium stabilized nitrogen rich α -sialons synthesized at 1500 °C are summarized in Table 3. The two-phase sample (Ca-0.2), having α - and β -sialon phases, displays a hardness of 18.5 GPa and fracture toughness of 4.5 $\text{MPa}\cdot\text{m}^{1/2}$. The HV_{10} of the single-phase α -sialon samples (Ca-0.6–Ca-1.4) is found to be in the range of 21.0–22.4 GPa and the fracture toughness is measured to be in the range of 5.6–6.1 $\text{MPa}\cdot\text{m}^{1/2}$. The presence of elongated morphology of α -sialon grains for samples having higher x value (i.e., more Ca_3N_2) may well be attributed to the formation of a higher amount of transient liquid phase. With not much of a difference, the highest fracture toughness of the sample Ca-1.6 is attributed to the relatively elongated morphology of α -sialon. For samples having x value greater than 1.6, a gradual decrease in the hardness is observed primarily due to the formation of CaSiAlN_3 and the presence of AlN

phases along with the major α -sialon phase. For a sample having 14 wt% AlN phase and 86 wt% CaSiAlN₃ phase, Cai [24] has reported a Vickers hardness of 14.4 GPa while Witek *et al.* [43] have reported a hardness of 12 GPa for hot-pressed AlN ceramics. The formation of multiple phases (having lower hardness) along with the gradual increase in grain size of the α -sialon phase is thought to have contributed towards the gradual decrease in the hardness.

HV_{10} values in the range of 16–20 GPa and fracture toughness of 3–7 MPa·m^{1/2} has been reported in the literature for the single or multi-cation calcium stabilized oxygen rich α -sialons [11,22,38,44,45]. In our study, the relatively higher measured hardness may well be attributed to the nitrogen rich α -sialons. The observation is in line with a study performed by Lofaj *et al.* [46], revealing that a 4% increase in N content would result in nearly the same increase in micro-hardness of RE–Si–Mg–O–N systems.

4 Conclusions

Calcium stabilized nitrogen rich sialon having compositions along the Si₃N₄:1/2Ca₃N₂:3AlN line were synthesized. Enhanced reaction kinetics due to nano/submicron-sized precursors and high heating rates achieved with the aid of the non-conventional SPS process allowed the preparation of well-densified nitrogen rich sialon ceramics at relatively low temperatures (1500 °C as compared to 1700 or 1800 °C). α -sialon phase for samples having Ca content (x) in the range of 0.15 < x < 1.83 was obtained. Formation of single phase nitrogen rich α -sialons was achieved for samples having nominal x value in the range of 0.4 < x < 1.6. An increase in the lattice parameters of α -sialon unit cell was observed to have a linear relationship with the amount of Ca²⁺ ions incorporated in the α structure. Increasing x value resulted in an increase in the average grain size from 286 to 468 nm.

Moreover, a higher amount of Ca₃N₂ starting powder was observed to facilitate the formation of elongated α -sialon grains. Calcium stabilized nitrogen rich sialon ceramics having very promising hardness and fracture toughness of 22.4 GPa and 6.1 MPa·m^{1/2}, respectively, were developed. Furthermore, the absence of a glassy grain boundary phase in nitrogen rich sialons makes them potentially viable candidates for high-temperature applications. It is believed that such engineering

ceramic materials would appeal to the ceramics industry owing to their unique properties and relatively low processing temperatures.

Acknowledgements

The authors would like to acknowledge the support provided by both King Fahd University of Petroleum and Minerals, Saudi Arabia, and the University of Sharjah, United Arab Emirates.

References

- [1] Sun WY, Tien TY, Yen TS. Subsolidus phase relationships in part of the system Si, Al, Y/N, O: The system Si₃N₄Al₂O₃Y₂O₃. *J Am Ceram Soc* 1991, **74**: 2753–2758.
- [2] Xie RJ, Hirosaki N, Sakuma K, *et al.* Eu²⁺-doped Ca- α -SiAlON: A yellow phosphor for white light-emitting diodes. *Appl Phys Lett* 2004, **84**: 5404–5406.
- [3] Grins J, Esmailzadeh S, Shen ZJ. Structures of filled α -Si₃N₄-type Ca_{0.27}La_{0.03}Si_{11.38}Al_{0.62}N₁₆ and LiSi₉Al₃O₂N₁₄. *J Am Ceram Soc* 2003, **86**: 727–30.
- [4] Suzuki S, Nasu T, Hayama S, *et al.* Mechanical and thermal properties of beta'-sialon prepared by a slip casting method. *J Am Ceram Soc* 1996, **79**: 1685–1688.
- [5] Izumi F, Mitomo M, Bando Y. Rietveld refinements for calcium and yttrium containing α -sialons. *J Mater Sci* 1984, **19**: 3115–3120.
- [6] Pomeroy MJ, Mulcahy C, Hampshire S. Independent effects of nitrogen substitution for oxygen and yttrium substitution for magnesium on the properties of Mg–Y–Si–Al–O–N glasses. *J Am Ceram Soc* 2003, **86**: 458–464.
- [7] Lavrenko VA, Gogotsi YG, Shcherbina OD. Kinetics and mechanism of oxidation of sialons. *Powder Metall Met Ceram* 1985, **24**: 710–713.
- [8] Persson J, Ekström T, Käll PO, *et al.* Oxidation behaviour and mechanical properties of β - and mixed α - β -sialons sintered with additions of Y₂O₃ and Nd₂O₃. *J Eur Ceram Soc* 1993, **11**: 363–373.
- [9] Liu LH, Xie RJ, Hirosaki N, *et al.* Photoluminescence properties of β -SiAlON: Yb²⁺, a novel green-emitting phosphor for white light-emitting diodes. *Sci Technol Adv Mater* 2011, **12**: 034404.
- [10] Wang PL, Zhang C, Sun WY, *et al.* Characteristics of Ca- α -sialon—Phase formation, microstructure and mechanical properties. *J Eur Ceram Soc* 1999, **19**: 553–560.
- [11] van Rutten JWT, Hintzen HT, Metselaar R. Phase formation of Ca- α -sialon by reaction sintering. *J Eur Ceram Soc* 1996, **16**: 995–999.
- [12] Riley FL. Silicon nitride and related materials. *J Am Ceram Soc* 2004, **83**: 245–265.
- [13] Hampshire S, Park HK, Thompson DP, *et al.* α' -Sialon ceramics. *Nature* 1978, **274**: 880–882.
- [14] Huang ZK, Greil P, Petzow G. Formation of alpha-Si₃N₄ solid solutions in the system Si₃N₄–AlN–Y₂O₃. *J Am*

- Ceram Soc* 1983, **66**: C–96–C–97.
- [15] Huang ZK, Tien TY, Yen TS. Subsolidus phase relationships in Si_3N_4 -AlN-rare-earth oxide systems. *J Am Ceram Soc* 1986, **69**: C–241–C–242.
- [16] Kuang SF, Huang ZK, Sun WY, *et al.* Phase relationships in the Li_2O - Si_3N_4 -AlN system and the formation of lithium- α -sialon. *J Mater Sci Lett* 1990, **9**: 72–74.
- [17] Huang ZK, Sun WY, Yan DS. Phase relations of the Si_3N_4 -AlN-CaO system. *J Mater Sci Lett* 1985, **4**: 255–259.
- [18] Herrmann M, Kurama S, Mandal H. Investigation of the phase composition and stability of the α -SiAlONs by the Rietveld method. *J Eur Ceram Soc* 2002, **22**: 2997–3005.
- [19] Kurama S, Herrmann M, Mandal H. The effect of processing conditions, amount of additives and composition on the microstructures and mechanical properties of α -SiAlON ceramics. *J Eur Ceram Soc* 2002, **22**: 109–119.
- [20] Sheu TS. Microstructure and mechanical properties of the *in situ* beta- Si_3N_4 /alpha'-SiAlON composite. *J Am Ceram Soc* 1994, **77**: 2345–2353.
- [21] Ekstrom T, Nygren M. SiAlON ceramics. *J Am Ceram Soc* 1992, **75**: 259–276.
- [22] Mandal H, Thompson DP. Sialon transformation in calcium-containing α -SiAlON ceramics. *J Eur Ceram Soc* 1999, **19**: 543–552.
- [23] Xie R, Mitomo M, Bando Y. Preparation of Ca- α -sialon ceramics with compositions along the Si_3N_4 -1/2 Ca_3N_2 : 3AlN line. *Z Met* 2001, **92**: 931–936.
- [24] Cai YB. Synthesis and characterization of nitrogen-rich calcium α -sialon ceramics. Ph.D. Thesis. Stockholm, Sweden: Stockholm University, 2009.
- [25] Wood CA, Zhao H, Cheng YB. Microstructural development of calcium alpha-SiAlON ceramics with elongated grains. *J Am Ceram Soc* 2004, **82**: 421–428.
- [26] Ye F, Hoffmann MJ, Holzer S, *et al.* Effect of the amount of additives and post-heat treatment on the microstructure and mechanical properties of yttrium- α -sialon ceramics. *J Am Ceram Soc* 2003, **86**: 2136–2142.
- [27] Shen ZJ, Peng H, Nygren M. Formation of *in situ* reinforced microstructure in α -sialon ceramics I: Stoichiometric oxygen-rich compositions. *J Mater Res* 2002, **17**: 336–342.
- [28] Cai YB, Shen ZJ, Grins J, *et al.* Self-reinforced nitrogen-rich calcium α -SiAlON ceramics. *J Am Ceram Soc* 2007, **90**: 608–613.
- [29] Information on https://en.wikipedia.org/w/index.php?title=Hot_pressing&oldid=827939071.
- [30] Information on http://www.fct-systeme.de/en/content/Spark_Plasma_Sinteranlagen/~nm.12~nc.26.
- [31] Khan RMA, Al Malki MM, Hakeem AS, *et al.* Development of a single-phase Ca- α -SiAlON ceramic from nanosized precursors using spark plasma sintering. *Mater Sci Eng: A* 2016, **673**: 243–249.
- [32] Camuşcu N, Thompson DP, Mandal H. Effect of starting composition, type of rare earth sintering additive and amount of liquid phase on $\alpha \rightleftharpoons \beta$ sialon transformation. *J Eur Ceram Soc* 1997, **17**: 599–613.
- [33] Ahmed BA, Hakeem AS, Laoui T, *et al.* Effect of precursor size on the structure and mechanical properties of calcium-stabilized sialon/cubic boron nitride nanocomposites. *J Alloys Compd* 2017, **728**: 836–843.
- [34] Irshad HM, Ahmed BA, Ehsan MA, *et al.* Investigation of the structural and mechanical properties of micro-/nano-sized Al_2O_3 and cBN composites prepared by spark plasma sintering. *Ceram Int* 2017, **43**: 10645–10653.
- [35] Al Malki MM, Khan RMA, Hakeem AS, *et al.* Effect of Al metal precursor on the phase formation and mechanical properties of fine-grained SiAlON ceramics prepared by spark plasma sintering. *J Eur Ceram Soc* 2017, **37**: 1975–1983.
- [36] Ahmed BA, Hakeem AS, Laoui T, *et al.* Low-temperature spark plasma sintering of calcium stabilized alpha sialon using nano-size aluminum nitride precursor. *Int J Refract Met Hard Mater* 2018, **71**: 301–306.
- [37] Information on http://www.chemicalbook.com/Chemical-ProductProperty_US_CB2672982.aspx.
- [38] Wang PL, Zhang C, Sun WY, *et al.* Formation behavior of multi-cation α -sialons containing calcium and magnesium. *Mater Lett* 1999, **38**: 178–185.
- [39] Eser O, Kurama S. A comparison of sintering techniques using different particle sized β -SiAlON powders. *J Eur Ceram Soc* 2012, **32**: 1343–1347.
- [40] Eser O, Kurama S. The effect of the wet-milling process on sintering temperature and the amount of additive of SiAlON ceramics. *Ceram Int* 2010, **36**: 1283–1288.
- [41] Hewett CL, Cheng YB, Muddle BC, *et al.* Thermal stability of calcium α -sialon ceramics. *J Eur Ceram Soc* 1998, **18**: 417–427.
- [42] Thorel A, Laval JY, Broussaud D. High temperature mechanical properties and intergranular structure of sialons. *J Phys Colloques* 1986, **47**: C1–353–C1–357.
- [43] Witek SR, Miller GA, Harmer MP. Effects of CaO on the strength and toughness of AlN. *J Am Ceram Soc* 1989, **72**: 469–473.
- [44] Xie ZH, Hoffman M, Cheng YB. Microstructural tailoring and characterization of a calcium α -SiAlON composition. *J Am Ceram Soc* 2004, **85**: 812–818.
- [45] Zhang Y, Cheng YB. Grain boundary devitrification of Ca α -sialon ceramics and its relation with the fracture toughness. *J Mater Sci Technol* 2003, **38**: 1359–1364.
- [46] Lofaj F, Dorcakova F, Kovalcik J, *et al.* The effect of lanthanides and nitrogen on microhardness of oxynitride glasses. *Kov Mater Mater* 2003, **41**: 145–157.

Open Access This article is licensed under a Creative Commons Attribution 4.0 International License, which permits use, sharing, adaptation, distribution and reproduction in any medium or format, as long as you give appropriate credit to the original author(s) and the source, provide a link to the Creative Commons licence, and indicate if changes were made.

The images or other third party material in this article are included in the article's Creative Commons licence, unless indicated otherwise in a credit line to the material. If material is not included in the article's Creative Commons licence and your intended use is not permitted by statutory regulation or exceeds the permitted use, you will need to obtain permission directly from the copyright holder.

To view a copy of this licence, visit <http://creativecommons.org/licenses/by/4.0/>.